3

THIRD GENERATION UED INSTRUMENTATION*

3.1 Introduction

Ultrafast electron diffraction combines several disparate fields of study: femtosecond pulse generation, electron beam optics, CCD detection systems, and GED. Output from a femtosecond laser is split into a pump path and an electron-generation path. The pump laser proceeds directly into the vacuum chamber and excites a beam of molecules. The probe laser is directed toward a back-illuminated photocathode, where the laser generates electron pulses via the photoelectric effect; the electrons are accelerated, collimated,

---

* Parts of this chapter have been adapted from Srinivasan, R.; Lobastov, V.A.; Ruan, C.-Y.; Zewail, A.H., *Helv. Chim. Acta*, **2003**, *86*, 1762.

focused, and scattered by the isolated molecules. The time delay between the arrival of the pump laser pulse and the probe electron pulse is controlled with a computer-driven translation stage. The resulting diffraction patterns are detected with a CCD camera, and the images are stored on a computer for later analysis. The UED-3 apparatus (Fig. 3–1) is also equipped with a time-of-flight mass spectrometer (MS-TOF) to aid in the identification of species generated during the course of chemical reactions. The following sections describe the individual components of the apparatus in more detail.

3.2 Femtosecond Laser System

The laser system can be divided into three stages: (1) ultrashort pulse generation, (2) pulse amplification, and (3) wavelength selection. In the first and second generations of UED, femtosecond laser pulses centered at 620 nm were generated with a home-built colliding-pulse, mode-locked ring dye laser (CPM) similar to the original system built for femtochemistry studies.[1, 2] Output from the CPM (100 MHz, 200 pJ) was amplified to 2 mJ in a 30-Hz, homebuilt, four-stage, NdYAG-pumped dye amplifier (PDA). The pump wavelength was either maintained at 620 nm or converted to 310 nm through second harmonic generation with a KD*P crystal. A wavelength of 258 nm was required to create photoelectrons from the gold photocathode. Therefore, part of the pump laser was focused into a quartz crystal to generate

continuum, and 516 nm was selected with a 10-nm bandpass filter. The energy of these pulses was then boosted to microjoules in a two-state, transversely-pumped dye amplifier. The amplified output was frequency-doubled with a BBO crystal to form ultraviolet light at 258 nm, and the final laser output was focused and directed toward the photocathode.

The femtosecond laser path in UED-3 is shown in Fig. 3–2. Femtosecond laser pulses (82 MHz, 8 nJ) centered at 800 nm are generated with a Ti:sapphire oscillator (Tsunami, Spectra-Physics). These pulses are then amplified in a 1-kHz two-stage Ti:sapphire amplifier (SuperSpitfire, Spectra-Physics) to yield an output pulse energy of 3 mJ. Both stages are pumped by 1-kHz intra-cavity doubled Nd:YLF lasers (Merlin, Spectra-Physics). Single-shot autocorrelation of the amplified pulses yields a pulse duration full-width at half-maximum (fwhm) of 120 fs. These pulses are frequency-tripled in a femtosecond third-harmonic generator (Uniwave Technology) to give UV femtosecond pulses (350 μJ, 267 nm). An optical beam splitter is used to split this UV output into two arms to form the pump beam and the electron generation beam. Most (90%) of the UV beam is directed into the scattering chamber to initiate the chemical reaction, whereas a smaller fraction of the laser power is directed into a delay line with a computer-controlled translation stage and then focused onto the photocathode in the electron gun.

3.3 Vacuum Chambers and Molecular Beams

The first-generation UED apparatus housed the electron gun, molecular beam, and the CCD detector in the same chamber. However, the electron gun was prone to arcing if the background pressure rose much above $1x10^{-4}$ Torr, and on at least one occasion, an electrical arc was strong enough to destroy a CCD. Keeping the electron gun clean and free from arcing was the motivation for introducing differential pumping in the second-generation apparatus, so that the electron-gun-chamber pressure could be kept below 1×10^{-6} Torr even while running sample gas in the scattering chamber at 1×10^{-4} Torr or higher.

The UED-3 apparatus (Figs. 3–3a and 3–3b) consists of four separate vacuum chambers—the electron gun, the scattering chamber, the detection chamber and the time-of-flight mass spectrometry chamber—in order to protect sensitive instruments from potentially corrosive sample molecules. Pressures below 1×10^{-7} Torr are attained in the scattering chamber in the absence of the molecular beam and are as high as 10^{-4} Torr when the molecular beam is operating. The pressure in the detection chamber is kept at 10^{-2} Torr to avoid condensation on thermoelectrically cooled surfaces. In an effort to minimize scattered light, the laser pulses enter the scattering chamber through a series of baffles attached to the light entrance port and exit through a Wood's horn sealed by a quartz window at Brewster's angle.

Care is taken to avoid any stray electric or magnetic fields that might distort the path of the scattered electrons.

The sample molecules enter the vacuum chamber in a free-jet expansion through a 125-μm diameter needle tip; the sample inlet manifold being mounted on a high-precision *xyz* positioning stage. The needle and inlet tube are wrapped with a resistive heating element to prevent condensation and clogging, while the sample bulb is warmed with heating tapes to provide sufficient vapor pressure of less volatile samples inside the chamber.

3.4 Electron Gun

In UED-3, the cylindrically symmetric gun consists of a negatively-biased photocathode, a gold extraction mesh, an aperture, and a magnetic focusing lens (Fig. 3–4). The electron gun, powered by a variable high-voltage power supply, is designed to operate at 30 kV (compared to 18 kV in UED-2). The photocathode is back-illuminated in this design: a thin, 450-Å silver film was deposited on one side of a sapphire window using a home-built metal evaporation chamber. A grounded gold extraction mesh, located 5 mm from the cathode surface, provides a very high extraction field of 6 kV/mm (compared to 2.7 kV/mm in UED-2) (see Fig. 3–5). The extracted electrons are then sent through a Pt:Ir aperture (150-μm diameter), which assists in cleaning the electron beam profile. The resulting equipotential lines in the

electron gun are shown in Fig. 3–6. In UED-2, a series of electrostatic lenses focused the electron beam by reducing the electron velocity over a region of several centimeters. However, replacing the electrostatic lens by a magnetic lens assembly (Fig. 3–7) in UED-3 successfully avoids this velocity reduction so that the electron velocity remains large and constant after the initial extraction, thereby reducing the transit time to the interaction region and concomitantly reducing the broadening of the electron pulse. Temporal characterization of the electron gun via a streak experiment is discussed in the next chapter. Two pairs of deflection plates provide x and y axis control of the electron beam, while a third pair of aluminum plates is used for streak measurements (Fig. 3–8).

3.5 CCD Camera System

A component critical to the success of UED is the detection system. The electron flux has to be maintained very low in order to keep the temporal resolution ultrafast. Early on, it was recognized that all of the scattered electrons must be detected for the experiment to succeed, and the two-dimensional CCD was introduced as a detector in direct electron bombardment mode in UED-1. To increase the longevity and flexibility of the detection system, UED-2 employed two CCDs: a small, direct-bombardment device installed in the scattering chamber for time-zero measurements, and

another large, scientific-grade device mounted in a separate chamber at the end of a phosphor scintillator/fiber optic/image intensifier chain for recording diffraction patterns.

In UED-3, we designed an improved low-noise, two-dimensional CCD camera assembly with the same elements as in UED-2, but without the small CCD (see Figs. 3–9 and 3–10). The camera has high detective quantum efficiency and principally comprises (Fig. 3–11) a phosphor scintillator (P-47), a fiber optic taper, a proximity-focused image intensifier (Hamamatsu), and finally the scientific-grade CCD camera (Photometrics, KAF-1000). Because the scattering intensity in electron diffraction decays rapidly with increasing scattering angle (usually varying over 6-8 orders of magnitude), we introduced a radially symmetric, variable neutral-density apodizing optical filter coated onto the backside of the scintillator—the rotating sector analog in our digital detection system, albeit with no mechanical moving parts. This filter allows the simultaneous measurement of diffracted intensities varying over 7 orders of magnitude, thereby effectively extending the dynamic range of detected intensities and consequently improving the precision of internuclear distance measurements in comparison with previous generations of UED. To block the scattered light and yet still permit single-electron detection, the phosphor screen is coated with 500-nm of aluminum.

The CCD chip consists of an array of 1024 x 1024 individual pixel elements (compared to 512 x 512 pixels in UED-2), each pixel being 24 μm on a side. The scattered electrons impinge upon a phosphor screen, thereby generating photons that are then transferred via a fiber-optic taper to a proximity-focused image intensifier. The photons are reconverted back to electrons at the photocathode on the front end of the image intensifier; the resulting electron signal is amplified and then reconverted back to photons at the back end of the intensifier. These photons are then transferred via a second fiber-optic taper onto the CCD chip.

Experiments showed that a single electron generates 20–30 counts, and saturation occurs above 65535 counts. The response of the CCD is linear over this range. The undiffracted beam, containing 99% of the electron intensity over a small area, is trapped by an aluminum beam stop mounted in front of the phosphor screen, in order to prevent damage. To enhance low-light sensitivity by reducing dark current, the CCD is cooled to –40˚C by a three-stage thermoelectric cooler, which is coupled to a liquid circulation heat exchanger to draw heat away from the thermoelectric cooler. The CCD chip is controlled with a camera electronics unit and a computer-driven digital imaging system (Roper Scientific, V++). The analog–digital conversion process operates with 16-bit resolution, and the readout rate is kept at 200 kHz to minimize digital noise. At this rate, a 512 x 512 pixel image (obtained

by operating the CCD in 2 x 2 binning mode) requires *ca.* 1 s for readout. The images are stored on a computer for subsequent data analysis. A typical experiment involves recording 1000 frames per second (kHz repetition rate) on the CCD over 240 s to give a single image that is readout in 1 s; *ca.* 100 such images are then averaged to produce the diffraction pattern at a specific time delay. The digital nature of our data acquisition permits the use of a variety of powerful image processing techniques that aid in the isolation of molecular diffraction signals, as detailed in the next chapter.

3.6 Time-of-Flight Mass Spectrometer

Unlike the previous generations of UED, UED-3 was also equipped with a time-of-flight mass spectrometer (TOF-MS), which could be used either in a linear arrangement or in a reflectron design. The schematic for the TOF-MS is shown in Fig. 3–12, while Fig. 3–13 shows the TOF-MS chamber. As UED-3 was designed to handle large and complex chemical and biological molecules, the TOF-MS was included in the design to help identify the different species that were being generated in the interaction volume, and hence to potentially narrow the search space for structural determination. As seen in Fig. 3–14, the TOF-MS consists of a set of retractable field plates and an MCP detector. The SIMION calculations of equipotential lines along the center plane are displayed in Fig. 3–15. Figure 3–16 shows the

synchronization of electrical pulses in the UED-3 TOF-MS setup and a typical mass spectrum for the $C_2F_4I_2$ is shown in Fig. 3–17. Note, however, that for all the systems reported in this thesis, the diffraction patterns alone were able to identify the structural species, and hence, there was no need to record the mass spectra. However, current efforts in UED-3 are focused on biological molecules, and the mass spectral information could play an important role in species identification in such cases.

References

1. Zewail, A. H., *J. Phys. Chem. A* **2000,** *104*, 5660.
2. Williamson, J. C. Ultrafast Gas-Phase Electron Diffraction. Ph.D. Thesis, California Institute of Technology, Pasadena, 1998.

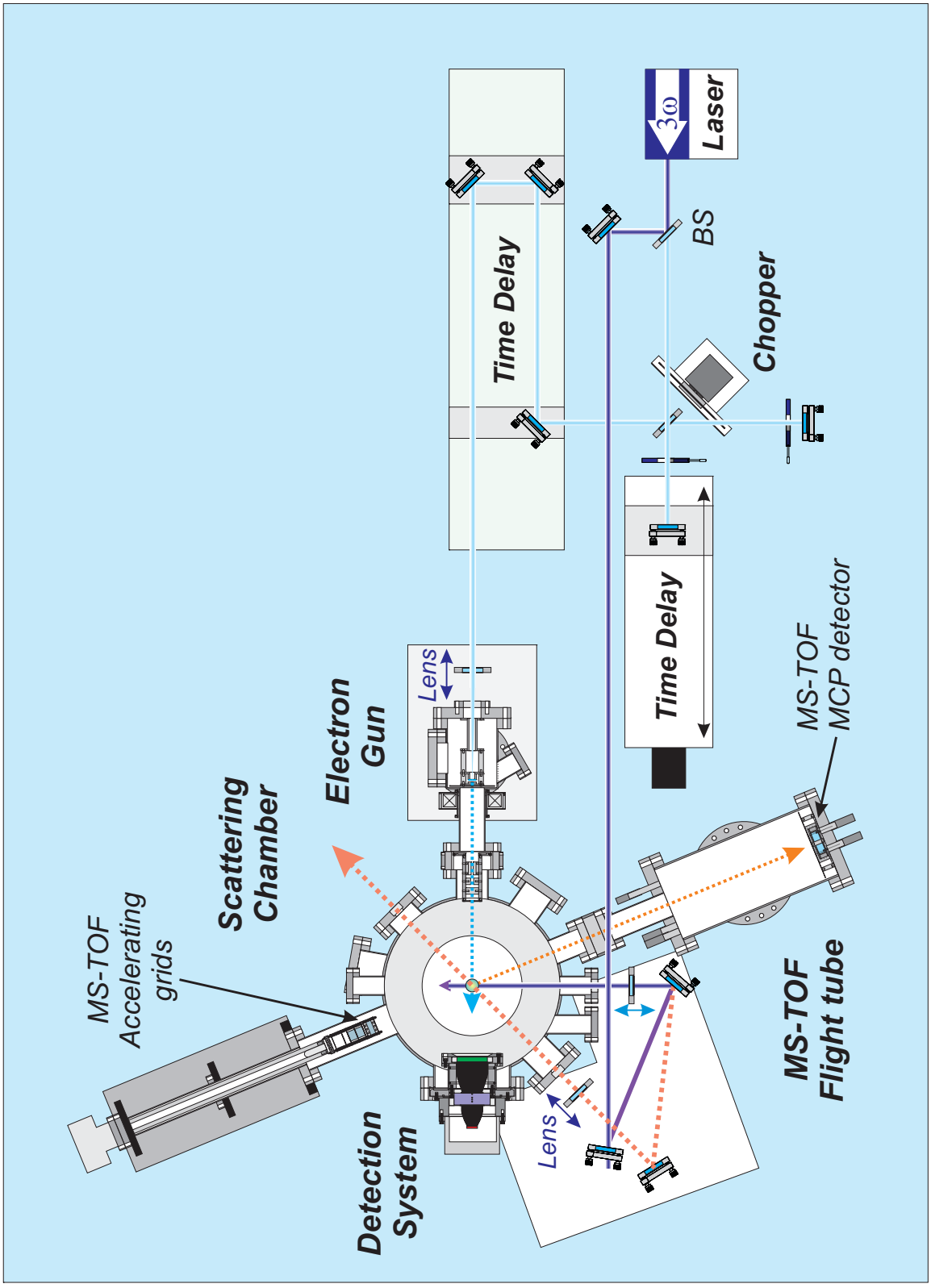

Figure 3-1. Third-generation UED-3 apparatus schematic, with the time-of-flight mass spectrometer (MS-TOF).

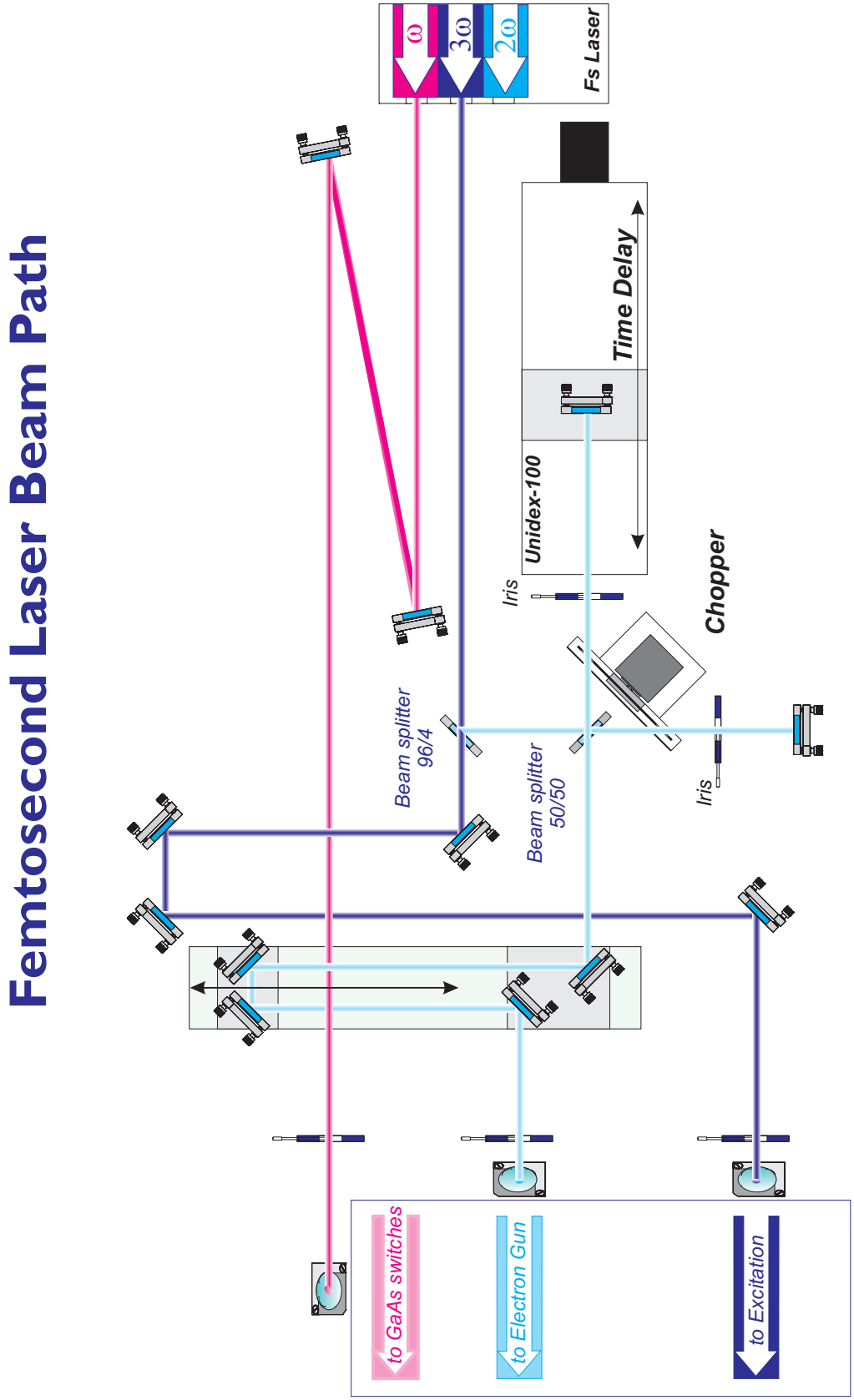

Figure 3-2. Layout of the beam path for the femtosecond laser pulses.

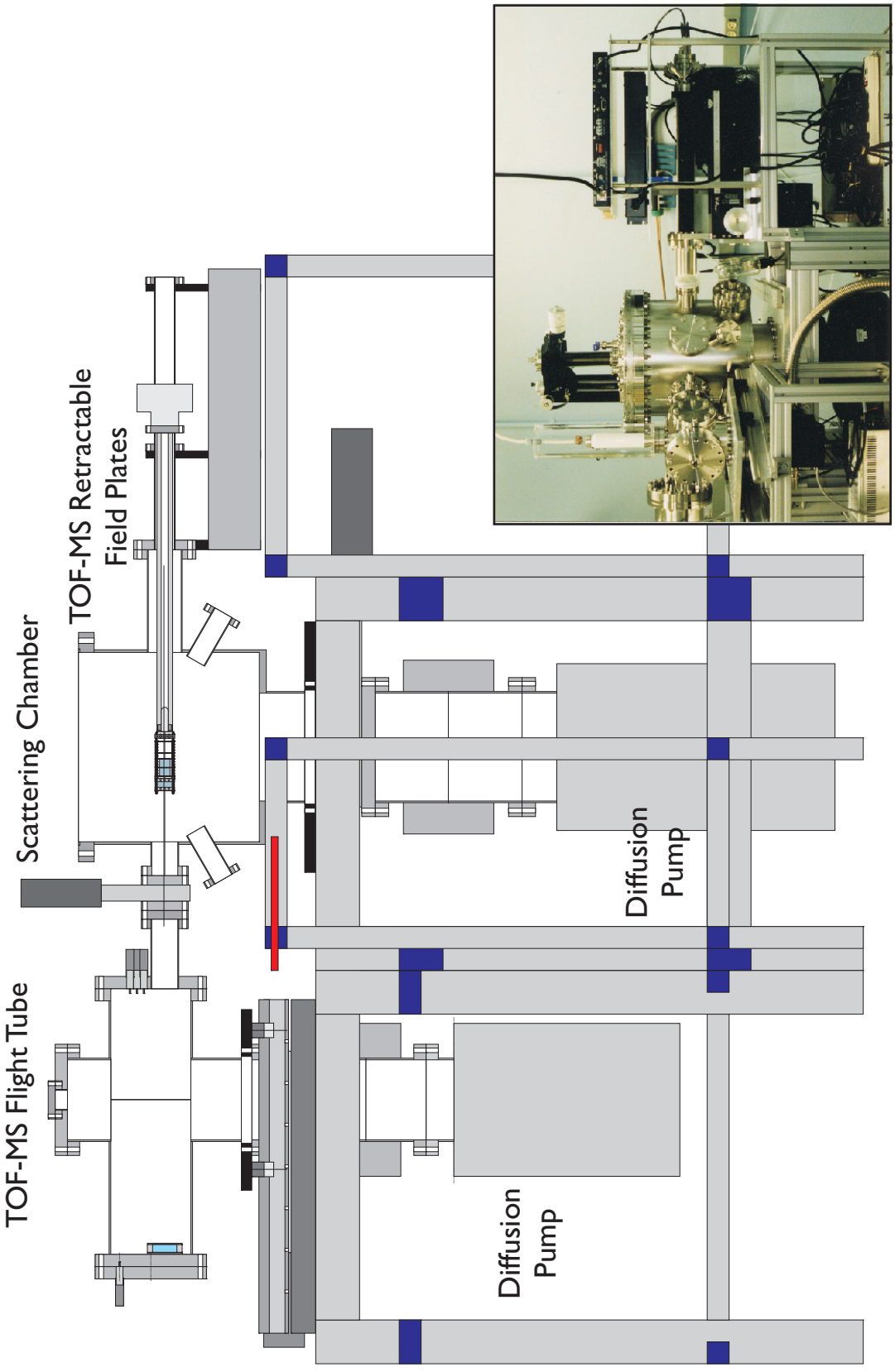

Figure 3-3a. Schematic front view of the UED-3 apparatus. Inset shows the photograph of the actual machine.

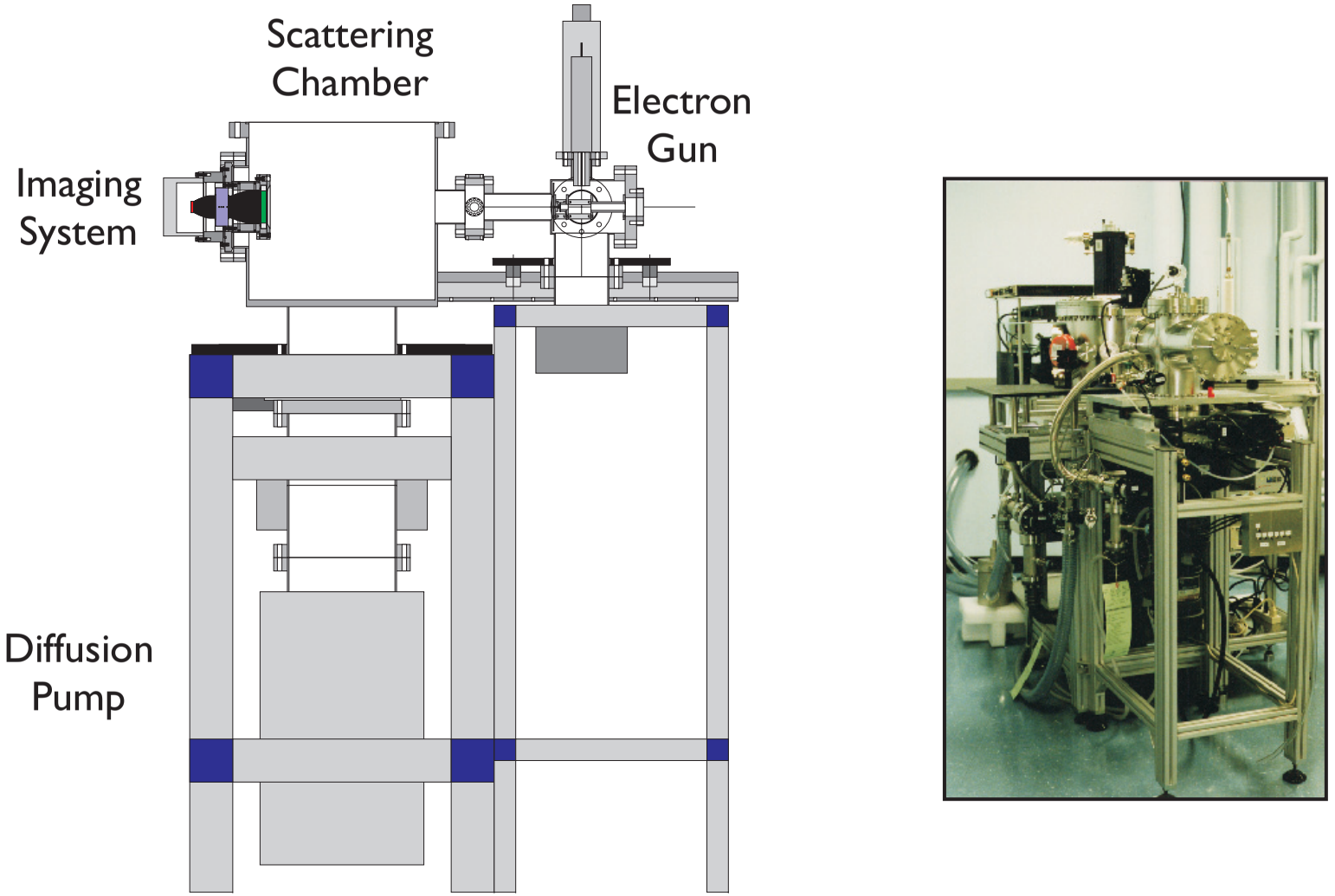

Figure 3-3b. Schematic side view of UED-3 apparatus. Also shown is the photograph of the diffraction machine.

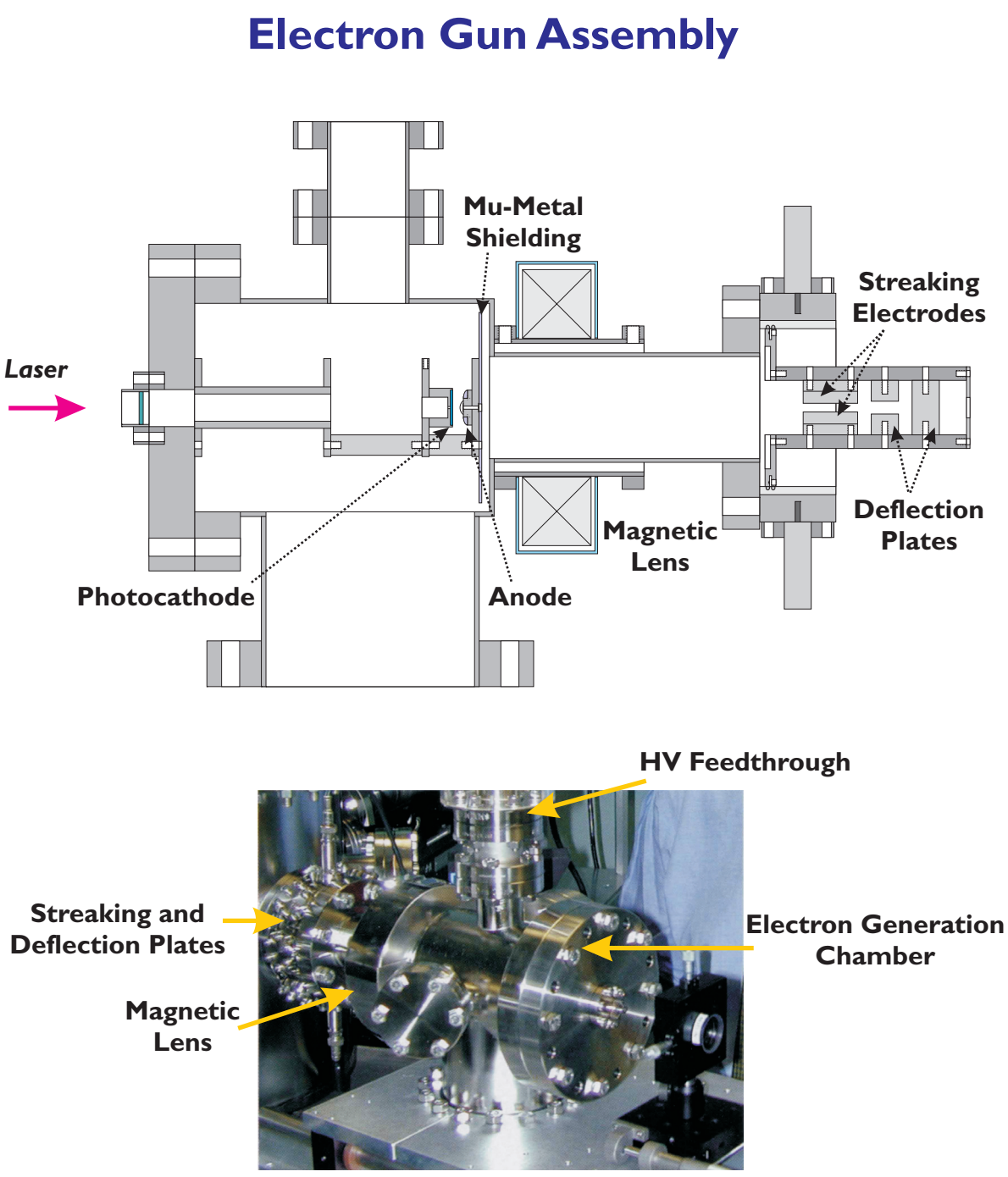

Figure 3-4. Schematic of UED-3 electron gun assembly. Also shown is a photograph of the electron generation chamber.

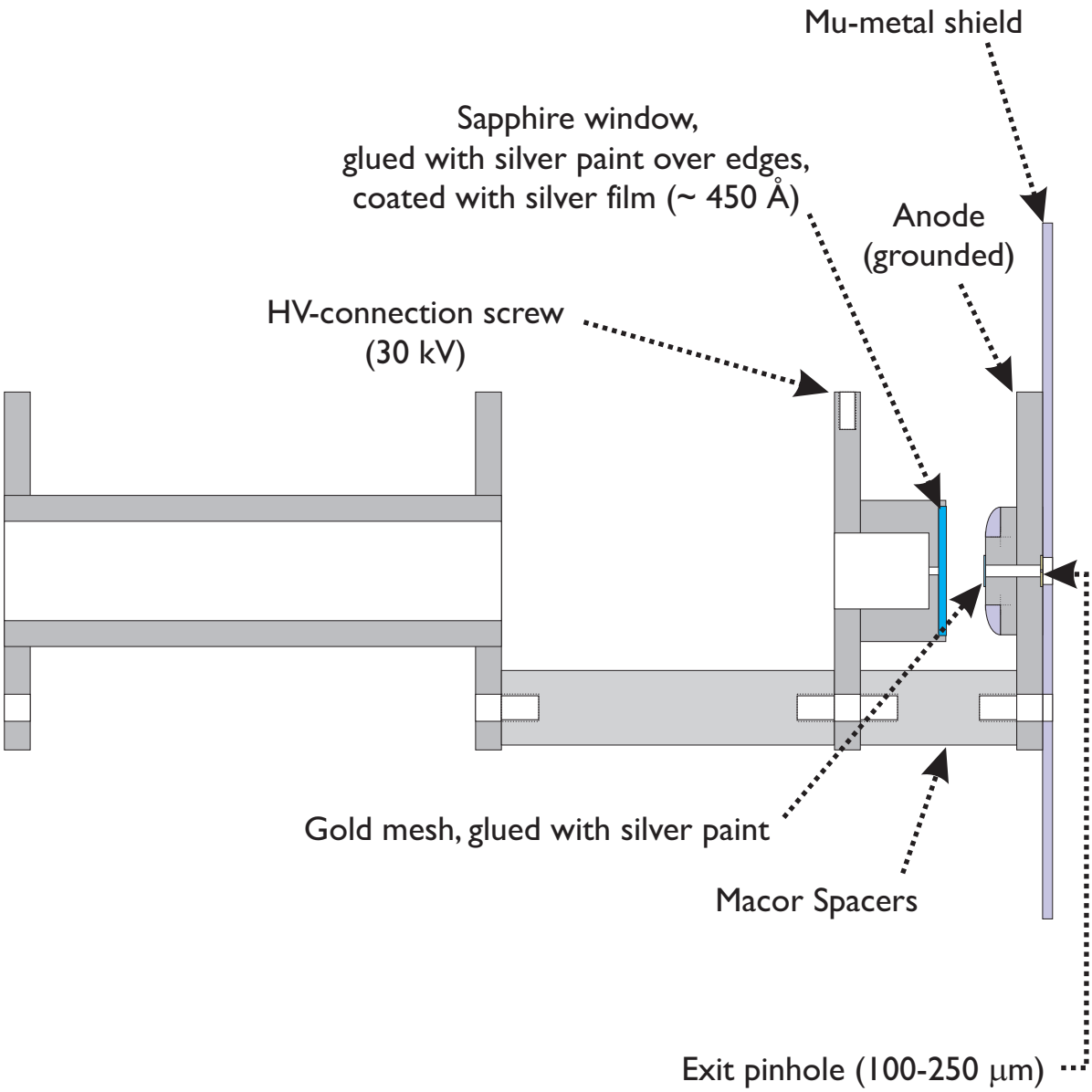

Figure 3-5. Detailed view of the electron generation and acceleration assembly.

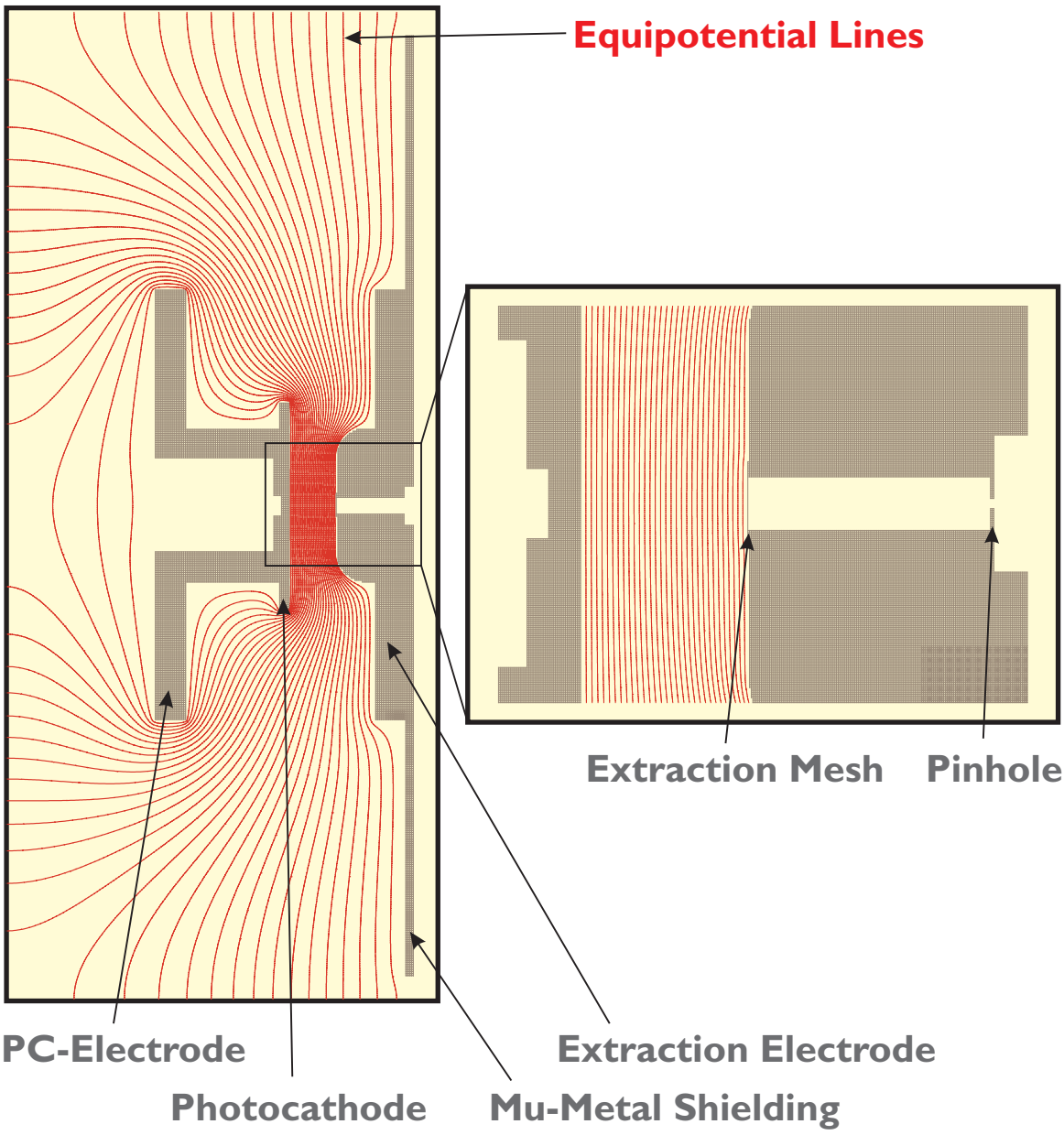

Figure 3-6. Equipotential lines in the extraction region of the UED-3 electron gun at 30 kV accelerating voltage.

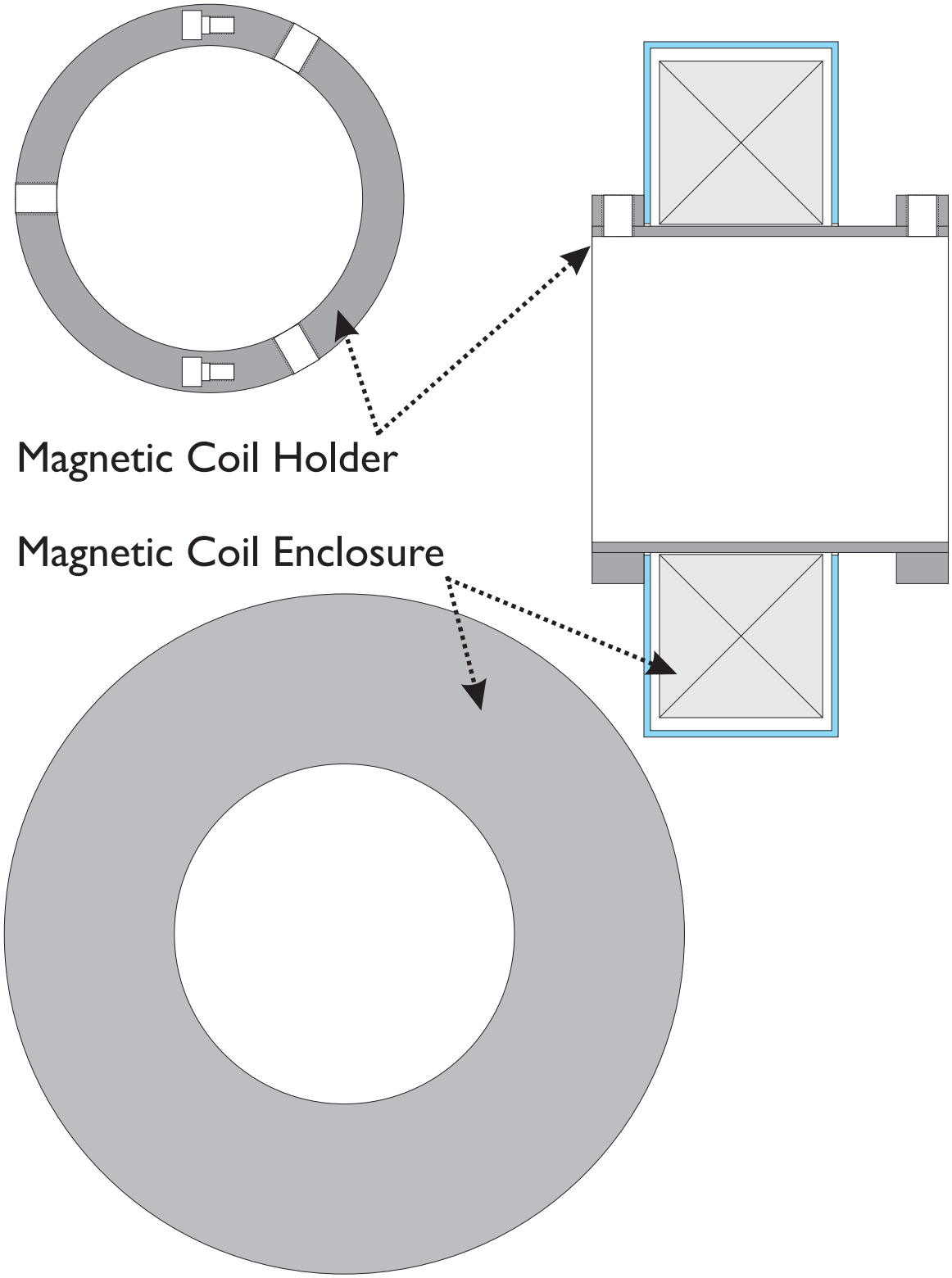

Figure 3-7. Detailed view of magnetic lens assembly.

Streaking and Deflection Assembly

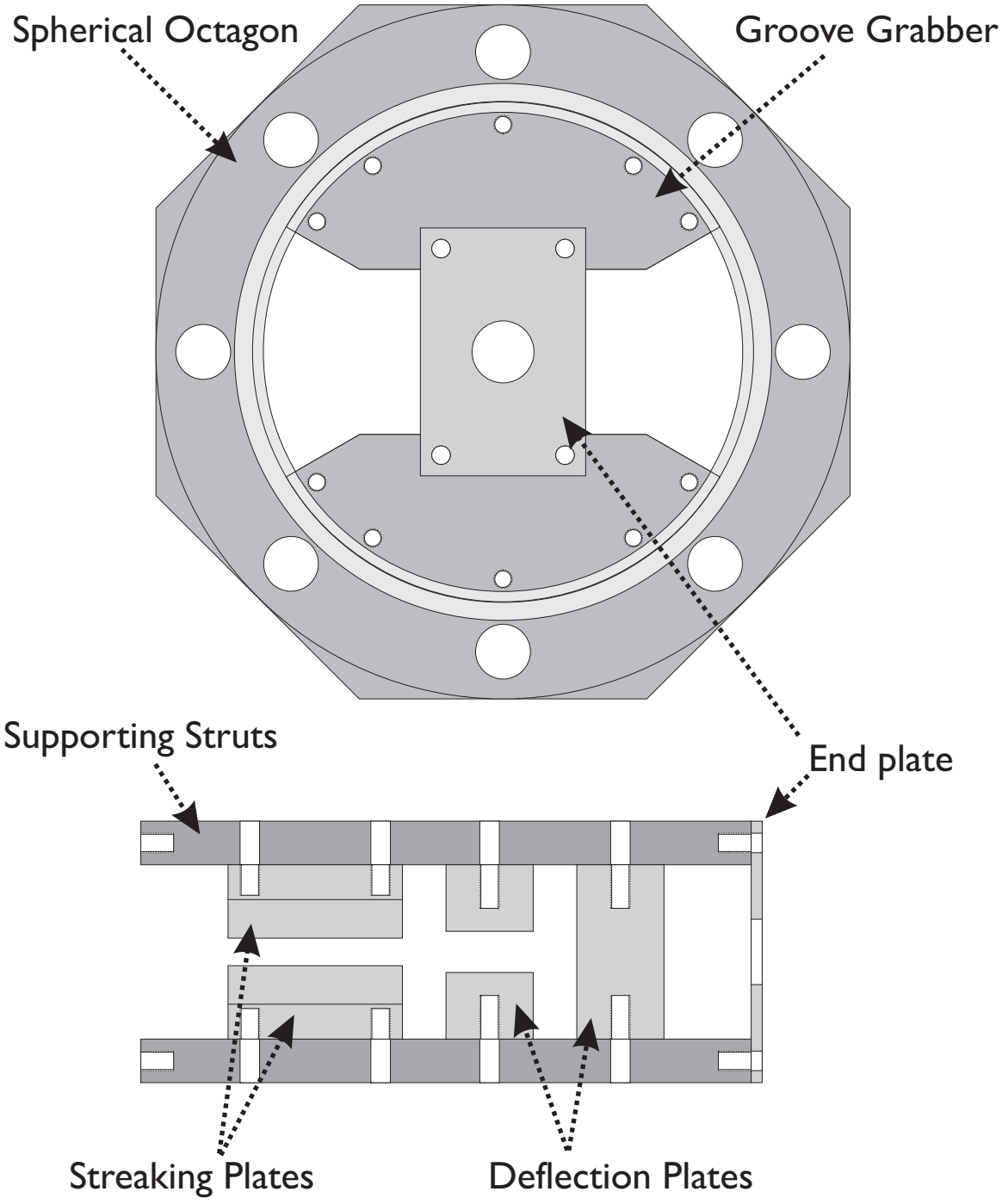

Figure 3-8. Detailed view of the electron streaking and deflection assembly.

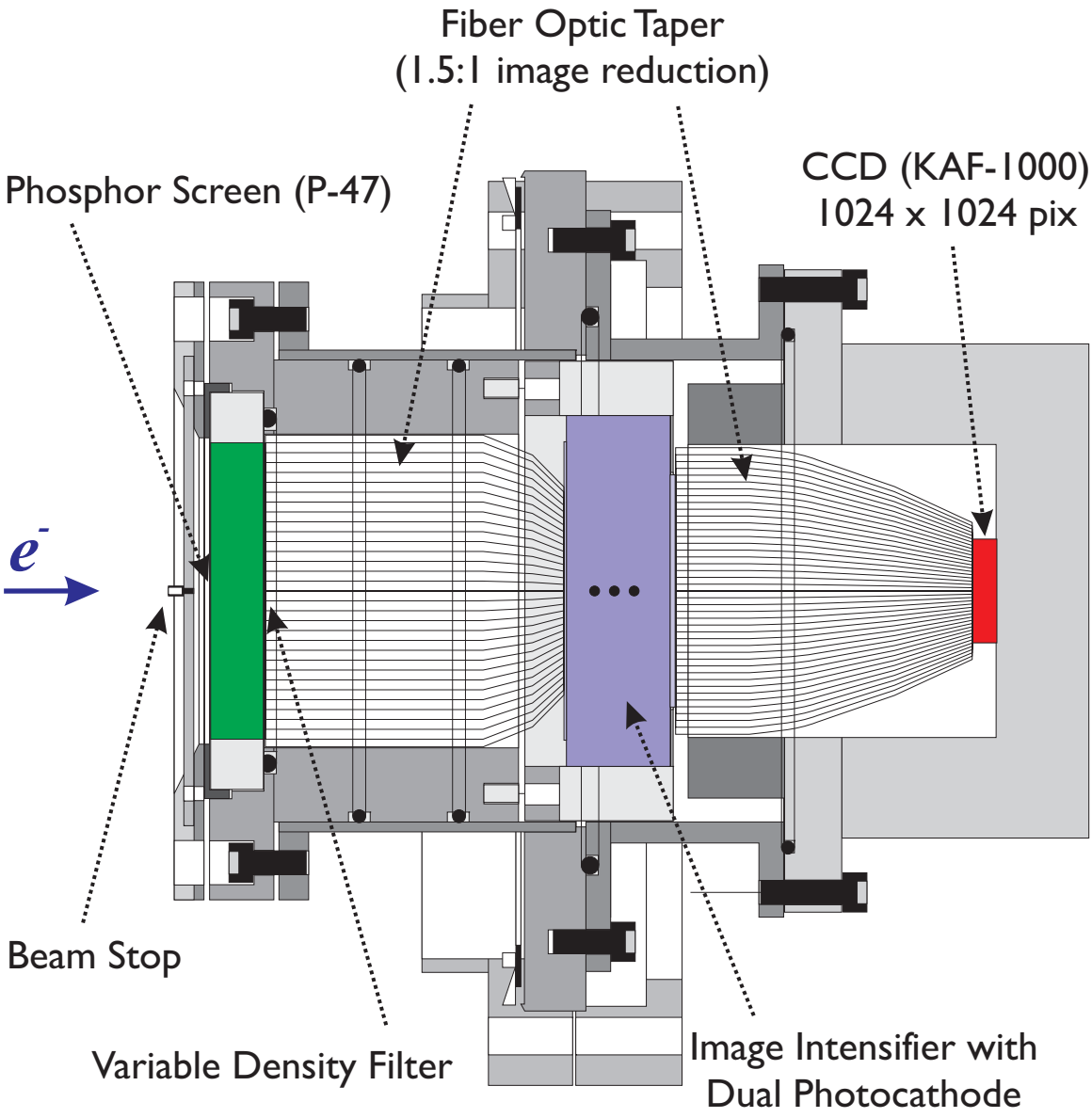

Figure 3-9. UED-3 Detector Assembly.

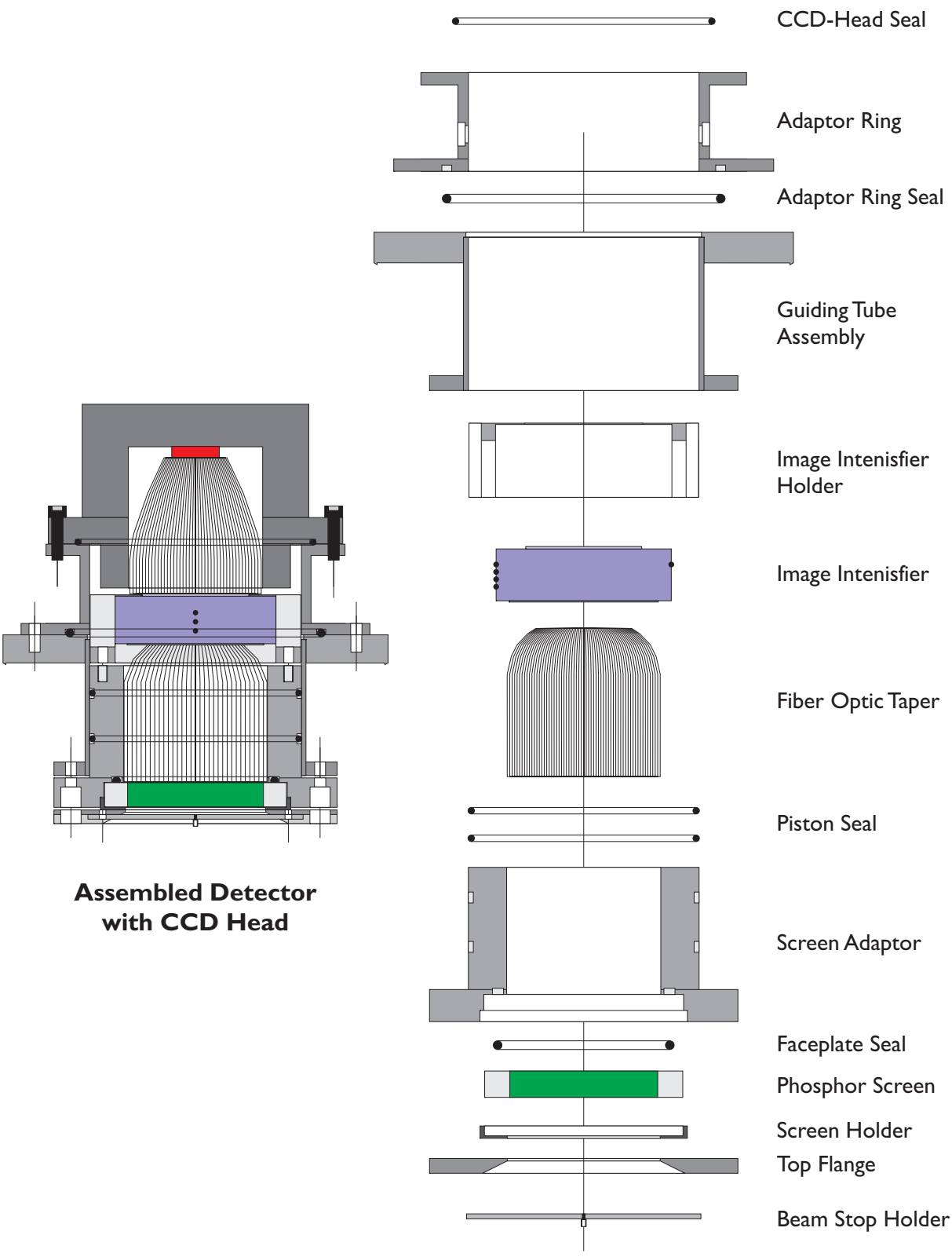

Figure 3-10. Individual components of the custom-made detector assembly.

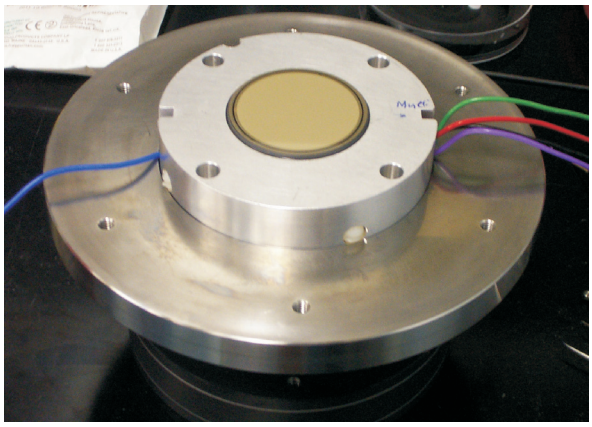

Image Intensifier

Fiber Optic Taper

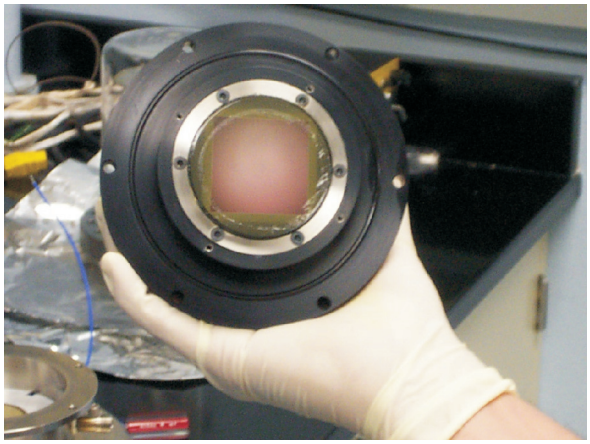

CCD Head

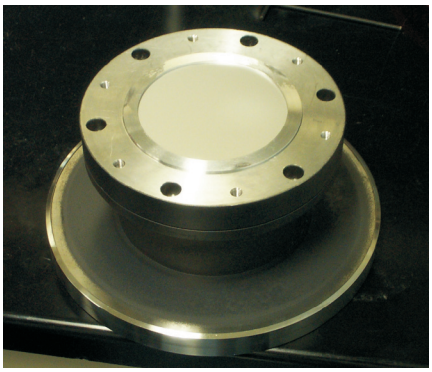

Phosphor Screen

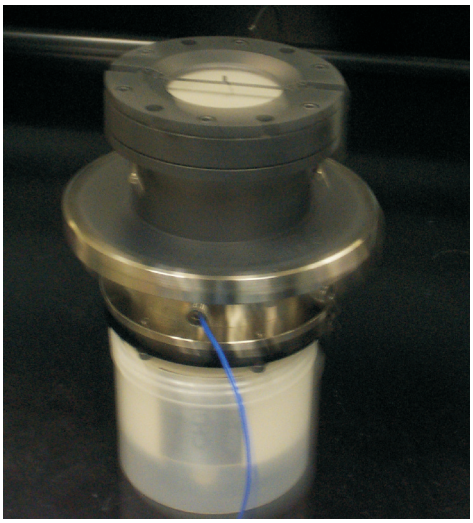

Fully Assembled Detector

Figure 3-11. Photographs of selected detector components.

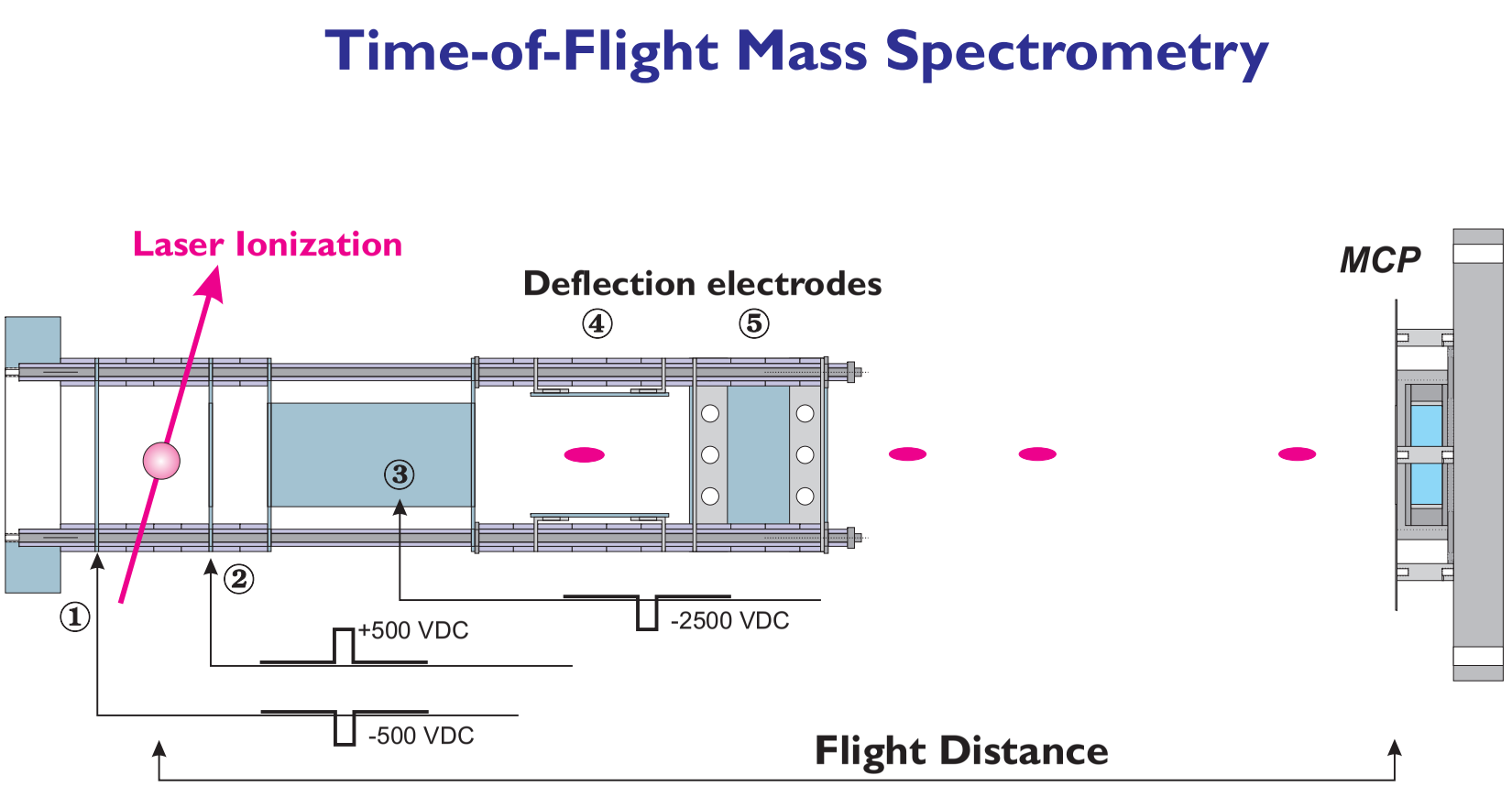

Figure 3-12. Schematic of time-of-flight mass spectrometry apparatus in UED-3. Also indicated are the applied electrical pulses; for details of the electrical arrangement and synchronization, see Figure 3-16.

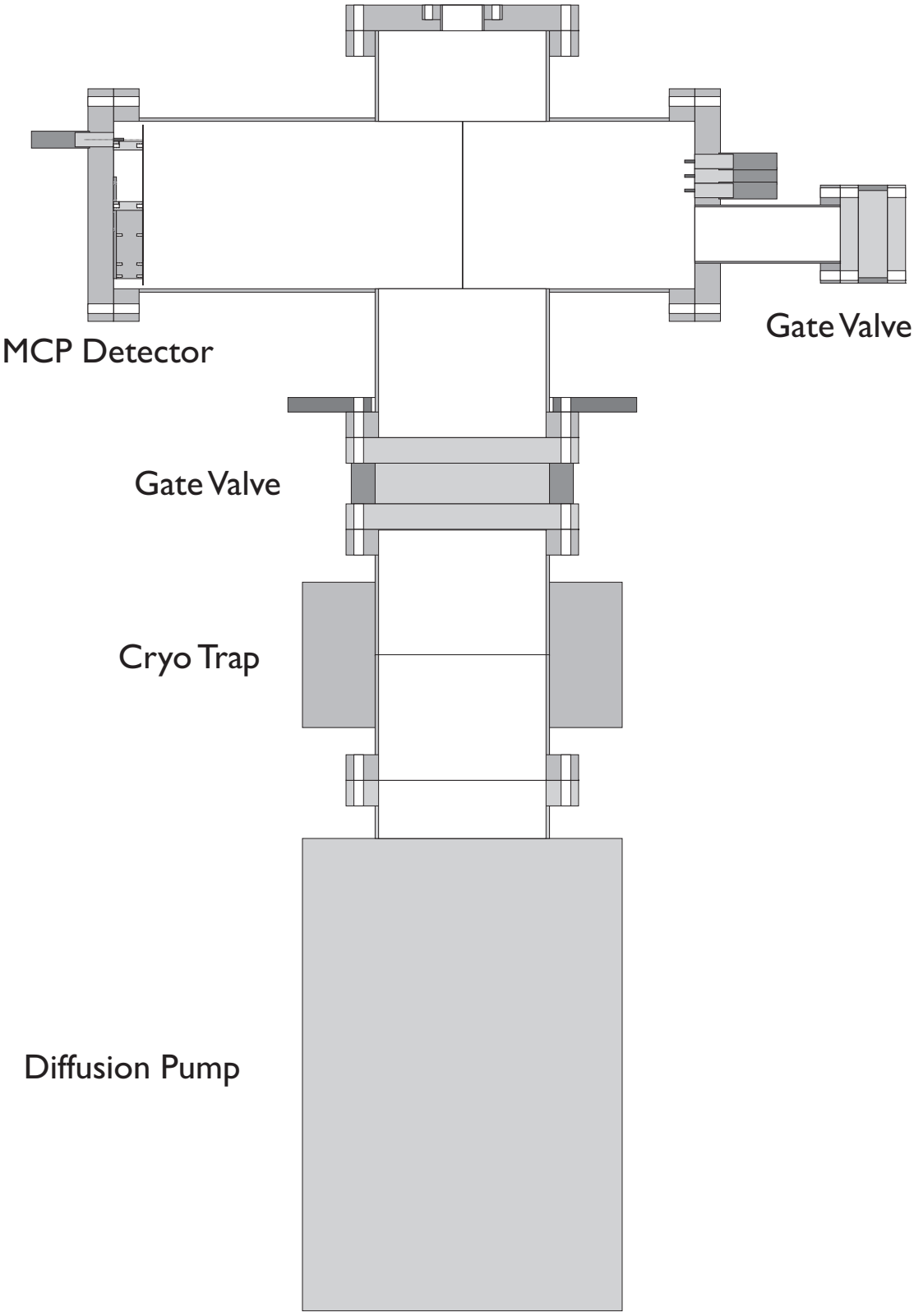

Figure 3-13. The linear TOF-MS chamber.

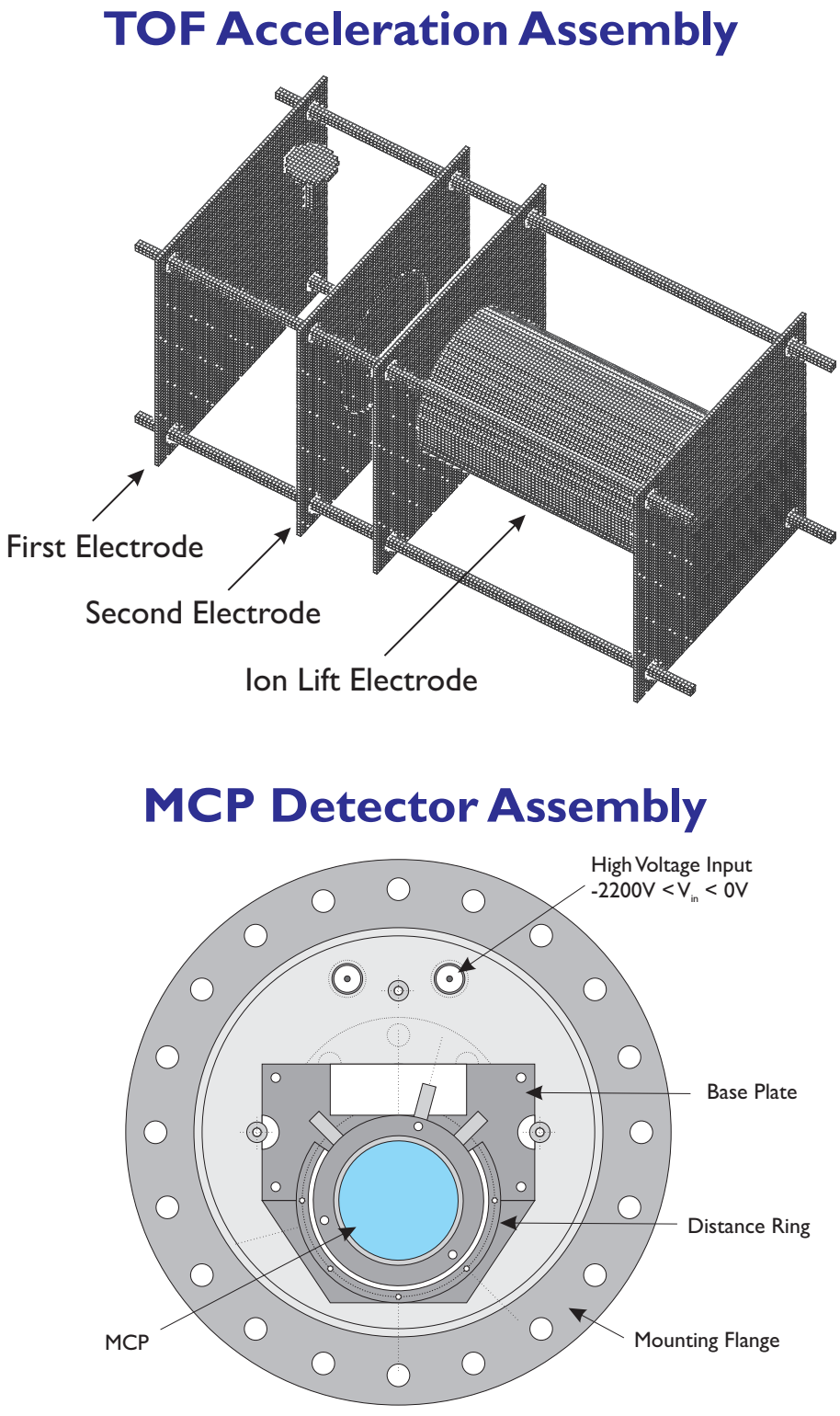

Figure 3-14. Acceleration assembly (top) and detector assembly (bottom) for time-of-flight apparatus.

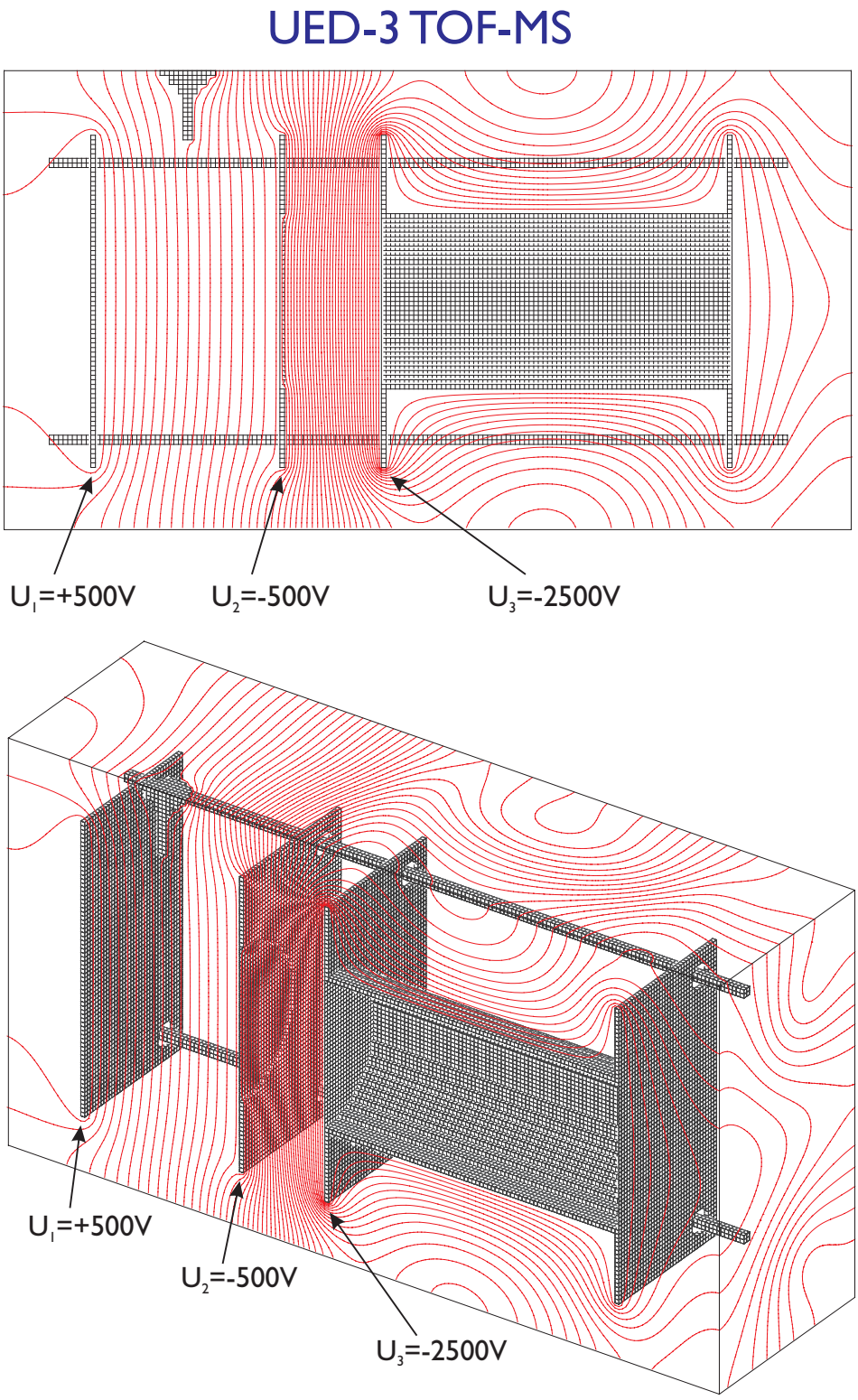

Figure 3-15. UED-3 geometry of time-of-flight mass spectrometry. Shown are equipotential lines along the center plane. Note the applied uniform acceleration fields and the nearly parallel equipotential surfaces.

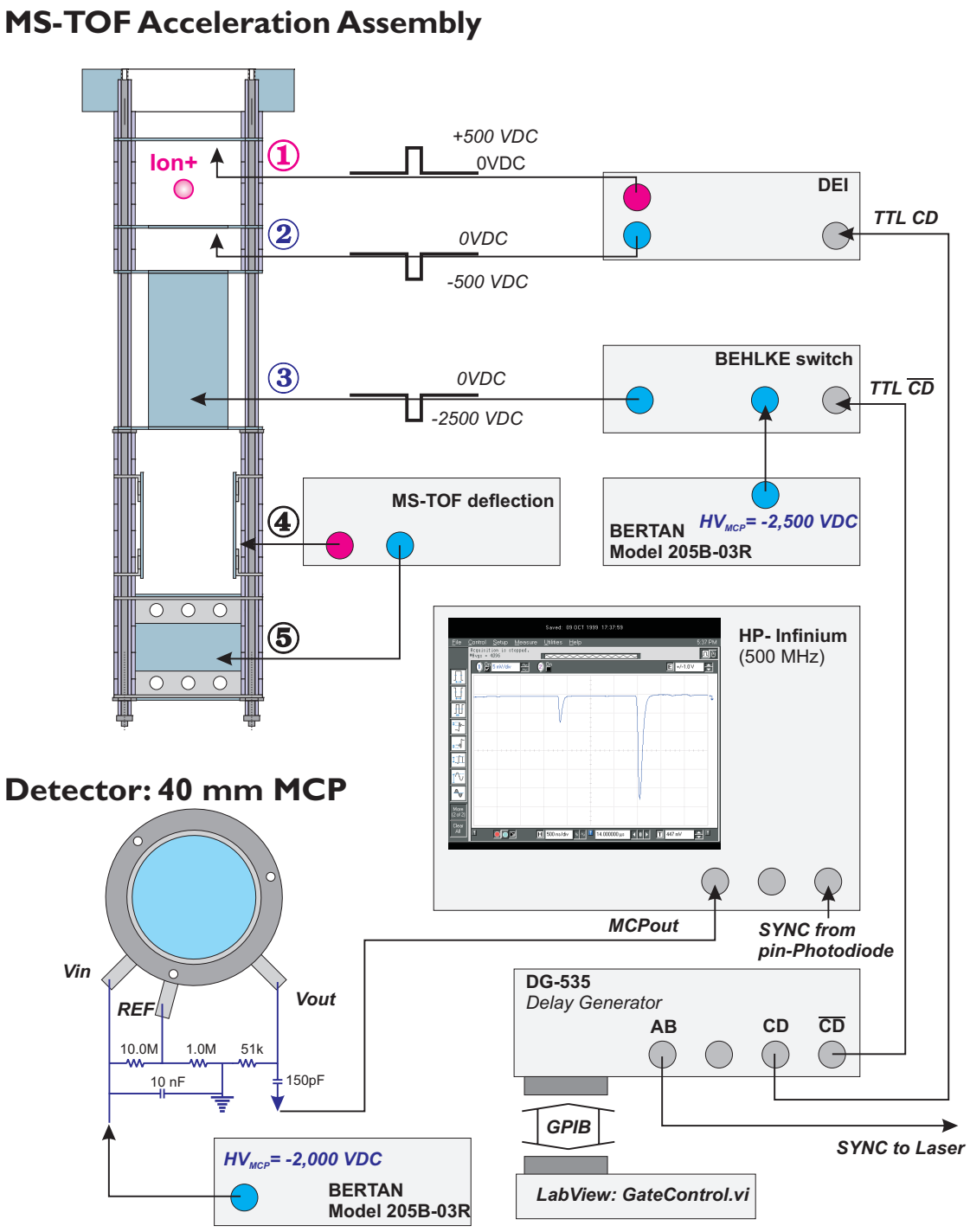

Figure 3-16. Arrangement and synchronization of electrical pulses in UED-3 time-of-flight mass spectrometry.

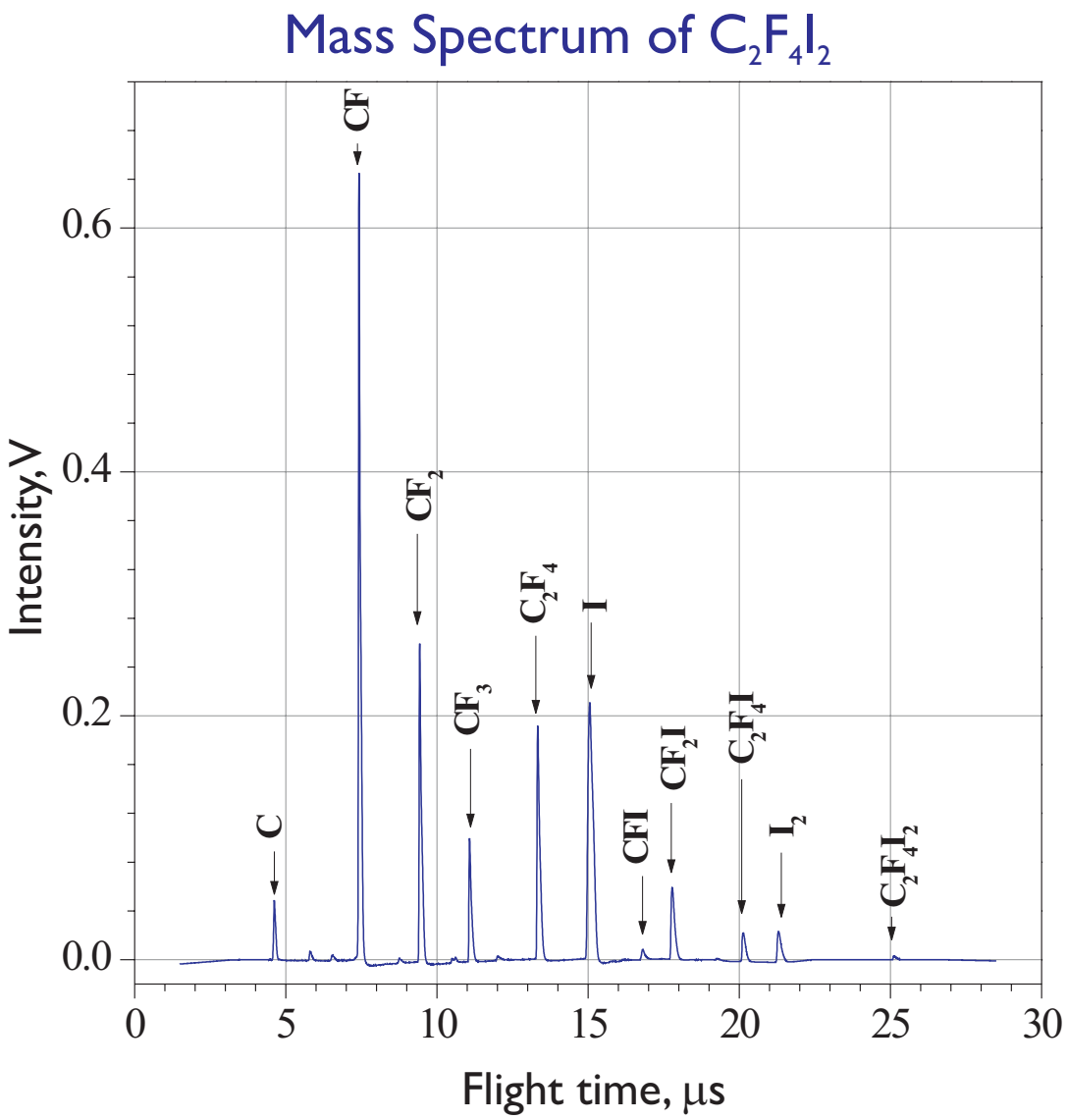

Figure 3-17. Typical mass spectrum obtained in the UED-3 time-of-flight mass spectrometry apparatus.